Influence of the thermomechanical processing on the superplastic forming of Mg-Al alloys

M.T. Pérez-Prado[1,*], J.A. Del Valle[1], F. Salort[1,+], F. Peñalba[2], X. Gómez[2], O.A. Ruano[1]

1 Dept. of Physical Metallurgy, Centro Nacional de Investigaciones Metalúrgicas (CENIM), CSIC, Avda. Gregorio del Amo, 8, 28040 Madrid, Spain

2 Fundación INASMET, Mikeletegi Pasealekua, 2, 20009 San Sebastián, Spain

* Corresponding autor. Phone: +34 91 5538900; email: tpprado@cenim.csic.es

+ Now at Initec, S.A.

Abstract

The aim of this paper is to study the influence of the initial microstructure of several Mg-Al alloys on their superplastic formability and on their post-forming microstructure and mechanical properties. Various thermomechanical processing routes, such as annealing, conventional rolling, severe rolling and cross rolling, were used in order to fabricate AZ31 and AZ61 alloys with different grain sizes. These materials were then blow-formed into a hat-shaped die. It was found that the processing route has only a small effect in the formability of Mg-Al alloys or on the post-forming microstructures and properties due to rapid dynamic grain growth taking place at the forming temperatures. Nevertheless, good formability is achieved as a result of the simultaneous operation of grain boundary sliding and crystallographic slip during forming.

Keywords: Mg alloys, superplastic forming, severe rolling.

1. Introduction

Magnesium alloys are attractive materials for structural and biomedical applications owing to their very small density (1.7 g/cm^3), only somewhat higher than that of plastics [1-4]. However, these materials exhibit low room temperature ductility due to the lack of a sufficient number of active slip systems and thus Mg parts are usually fabricated by casting and extrusion [5-8]. Alternative high temperature technologies, such as thixoforming and superplastic forming, are also envisioned as potentially viable routes for the fabrication of Mg parts [9]. In particular, superplastic forming, consisting on applying a hot air pressure on a sheet until it adopts the shape of a customized mould, allows producing homogeneous parts of complex shapes in one single operation [10].

It is well known that superplasticity takes place preferentially in fine-grained materials ($d < 10$ μm) [10,11]. A number of studies have thus been carried out over the past few years with the aim of developing thermomechanical processing routes for grain refinement in Mg alloys, in order to increase their superplastic formability [12-14]. Several reports have indeed demonstrated the superplastic formability of Mg alloys [15-20]. However, further research on the relationship between processing, microstructure and post-forming properties of these materials under different forming conditions is still needed.

The aim of this paper is to compare the formability as well as the post-forming microstructure and mechanical properties of AZ31 and AZ61 Mg-Al-Zn alloys with a wide array of starting microstructures, obtained by various processing routes such as annealing, conventional rolling, severe rolling, and cross rolling. The predominant deformation mechanisms during forming are investigated on the light of these findings.

2. Experimental procedure

The materials used for this study were the Mg alloys AZ31 (3%Al-1%Zn) and AZ61 (6%Al-1%Zn), provided by KG Fridman and Magnesium Elektron. The alloys were received in the following conditions: AZ31-O (rolled and annealed), AZ31-H (processed by conventional rolling, i.e., by means of small strain passes), AZ61-O (rolled and annealed). The AZ31-O and AZ61-O alloys were subsequently severely rolled (SR) at 400ºC using two passes with, respectively, 10% and 63% thickness reductions (AZ31) and 10% and 44% reductions (AZ61). The resulting microstructures will hereafter be called AZ31-SR and AZ61-SR. Additionally, the AZ61-O material was cross rolled (CR) at 375^{o}C using small strain passes (< 10% reduction per pass) up to a total thickness reduction of 50%. The final sheet thickness was 1.5 mm. This sample will be named AZ61-CR. Rolling was carried out in a Carl Wezer rolling mill, furnished with 13 cm diameter rolls rotating at 52 rev min^{-1}.

The materials described above [AZ31-O (1,6mm), AZ31-H (1,6mm), AZ31-SR (1 mm), AZ61-SR (1.5 mm), AZ61-CR (1,5mm)] were blow formed at 375ºC and 400ºC into hat-shaped dies (Figure 1) with ratios of 6 and 9 and using air pressures ranging from 0.8 to 1.6 MPa. Forming at lower temperatures proved technically impossible due to the high stress levels required. These forming conditions lie within the limits that are feasible at an industrial level [21]. The blow forming press, located at INASMET, San Sebastián, Spain. Several combinations of pressure, die radius and forming times were used in order to optimize the formability of the different alloys. The optimum conditions corresponding to each sample are summarized in Table 1. Best formability, defined as the capacity to better fill the mould without cracking, was obtained in all cases at 400ºC and predominantly using 9 mm die radii. This paper

focuses on the post-forming properties of the five samples described in Table 1 and Fig. 2.

The microstructure of the as-received, processed (rolled) and blow formed samples was examined by optical microscopy. Measurements in the former two were performed along the rolling plane. Two areas throughout the profile of the hat-shaped specimens were studied (Fig. 1), namely the "top of the hat" (zone A), where the highest deformations are attained, and the clamping region, where no deformation takes place (zone B). The area fraction of cavities was measured using the software for image analysis Image Tools 3.0. Sample preparation for cavity measurement included grinding with increasingly finer SiC papers and mechanical polishing with 6 μm and 1 μm diamond paste. The grain size was measured by the linear intercept method. Samples for grain size measurements required an additional chemical etching step with a solution of 0.5 g of picric acid, 0.5 ml of acetic acid, 1 ml of distilled water and 25 ml of ethanol in order to reveal grain boundaries. Special care was taken during sample preparation in order not to introduce twins during the different grinding and polishing steps. X-ray texture analysis was performed in zone A in both the as-processed and formed samples. The measurements were carried out in a Siemens D5000 diffractometer, furnished with a closed eulerian cradle, by means of the Schulz reflection method and using CuKα radiation. Five direct pole figures were measured, namely (0002), (10-10), (11-20), (10-11), (10-12).

The room temperature mechanical behavior of the processed and blow formed materials (zone A) was measured by means of uniaxial tensile tests performed at a strain rate of 10^{-3} s^{-1} in an electromechanical Servosis testing machine. Additionally, in order to explore the deformation mechanisms predominant during forming, strain rate change

tensile tests were also carried out at 400ºC. The testing temperature was reached using the same ramp as in the blow forming tests. It consisted on three steps: a temperature of 300ºC was first reached in 10 min., the temperature was increased to 400ºC in the next 5 min., and it was maintained during 10 more minutes before testing. From the strain rate change tests the stress exponent (n) and strain rate sensitivity (m) exponents were calculated. Flat tensile coupons of 15 mm gage length were cut out of the as-received and processed materials. Due to size limitations, the gage length of the tensile coupons cut out of the blow formed samples (zone A) was 9 mm. The width of these specimens was 3 mm. The radius was equal to 3 for all tensile specimens.

3. Results and discussion.

The microstructure of the as-received and processed Mg Alloys is illustrated in Figure 3 by means of optical micrographs. The corresponding grain size and shape data are briefly summarized in Table 2. In short, the AZ31-O alloy exhibits an equiaxed microstructure, characteristic of recrystallized materials; the AZ31-SR an AZ61-SR samples possess bimodal microstructures, with coarse grains embedded in a matrix of smaller, dynamically recrystallized grains [22]; the AZ31-H material has a typical fine deformation structure, formed by elongated grains; finally the AZ61-CR alloy is formed by equiaxed grains with a large fraction of twins. In spite of the significant differences in grain size and shape in the various materials under study, the texture of all the samples is very similar: the main component is a basal fiber, i.e., basal planes are oriented preferentially parallel to the rolling plane. The intensity at the center of the (0002) X-ray direct pole figure is shown in Table 2. In the following, the response of this wide range of microstructures to blow forming will be investigated.

The samples that exhibited the best formability, i.e., where complete filling of the mould was achieved without cracking, as well as the corresponding forming temperature, die radius and forming time, are listed in Table 1. This study will emphasize the post-forming properties of these specific samples.

Microstructure of the blow formed Mg-Al alloys

The post-forming microstructures of the materials with optimum formability are summarized in Table 3. In particular, the grain sizes corresponding to zones A and B are shown. Figure 4 illustrates the microstructure of the different blow formed samples. A comparison between the grain size values in the as-received and processed materials (Table 2 and Fig. 3) with those of the blow formed samples (Table 3 and Fig. 4) reveals that grain growth has taken place during forming.

Additionally, equiaxed microstructures develop in all the samples: the initially elongated structure of the AZ31-H alloy and the bimodal grain size distributions of the severely rolled samples disappear during forming. In order to determine to what extent grain growth takes place during deformation itself, i.e., under dynamic conditions, or during heating up to the forming temperature, annealing treatments emulating the temperature ramp utilized were performed. The resulting grain sizes are also summarized in Table 3. It can be seen that, except in the alloy AZ31O, significant grain growth takes place already during static heating for temperature stabilization. Grain size values are somewhat larger in zone B than in the annealed materials, since zone B was additionally exposed to static annealing at 400ºC during the blow forming time. No obvious evidence of strain induced grain growth is apparent. In fact, the grain size tends to be similar in the highly deformed areas (zone A) and in the non-deformed zones (B)

in most of the samples. The smallest grain size is observed in the alloy AZ31-H. The initial deformation structure of this alloy, typically formed by a large fraction of low to intermediate angle boundaries [23], is less prone to growth due to the smaller mobility of low angle boundaries. In all the other samples, the presence of a large fraction of high angle boundaries before forming favors faster dynamic grain growth at the forming temperatures. Twinning was observed in most of the samples, especially in the outer layer. This could be attributed to the presence of compression stresses once the materials become in touch with the mould.

Table 3 illustrates that the area fraction of cavities is, in general, larger in the highly deformed areas (zone A) than in those regions where no deformation was applied (zone B). Cavitation is often observed during superplastic deformation. Although the micromechanism governing superplastic deformation is still not clear [11], it has been proposed that, as a consequence of grain boundary sliding, high stresses may accumulate at triple points, which can not be relieved by a suitable accommodation mechanism,[10,11] and thus cavitation takes place. This observation is especially notable in the AZ61-CR alloy, where a very large fraction of cavities develop during superplastic forming. This may be attributed to the large initial grain size (28 μm, not counting twin boundaries, in the as-processed material and 36 μm in the annealed material, right before deformation begins) and to the unsuitability of twin boundaries (stable, low energy interfaces) for sliding.

Finally, texture measurements revealed that no appreciable changes in the texture occur during blow forming. In fact, in all the samples the main component is still a well-defined basal fiber texture. The X-ray intensity at the center of the (0002) pole figure, corresponding to each sample, is listed in Table 3. Superplastic deformation

is usually associated with texture randomization [10]. Grain boundary sliding (GBS) causes random grain rotations and this leads to a decrease in the texture intensity. In the present study, however, the post-forming textures are either equally strong or even slightly stronger than the initial textures. This suggests that other mechanisms, such as crystallographic slip (CS) -that, acting alone, leads to the stabilization of specific texture components [24] may contribute to deformation.

Mechanical properties of the blow formed Mg-Al alloys

Ideally, superplastically formed materials should retain the strength and ductility levels of the corresponding starting materials. However, this is rarely the case. In order to evaluate the degradation in the room temperature mechanical behavior of the Mg-Al alloys under study, tensile tests were performed at 10^{-3} s^{-1}. Figure 5a illustrates a comparison between the maximum flow stress and the elongation to failure. Blow forming leads to a decrease in the maximum flow stress of all the materials investigated due, mostly, to the increase in grain size. The strength decrease is, however, more noticeable in the AZ61 alloys than in the AZ31 materials for similar relative grain size increases. The difference may be attributed to the dissolution of the β-phase particles, presumably present to a larger extent in the AZ61 alloy due to the larger amount of Al, during forming at 400ºC. Figure 3b illustrates the ductility of all the samples investigated, both before and after blow forming. Ductility decreases in all samples except in AZ31-O and AZ61-LS.

Figure 6 shows the strain rate versus stress data corresponding to tests performed at 400ºC. These testing conditions resemble the deformation conditions during blow forming. Two regimes can be clearly distinguished: at strain rates higher than about

$5x10^{-4}$ s^{-1}, the stress exponent (n) is ~4. This is consistent with dislocation movement being the predominant deformation mechanism. At strain rates lower than $5x10^{-4}$ s^{-1} n is ~2, which has been associated to grain boundary sliding dominated deformation. During blow forming, the approximate strain rate is close to $5x10^{-4}$, i.e., the deformation conditions are in the proximity of the transition between the two regimes described above.

Deformation mechanisms responsible for superplasticity during blow forming

Several observations point toward the coexistence between grain boundary sliding and dislocation movement during blow forming of the Mg-Al alloys studied. First, if GBS were the only deformation mechanism, texture randomization would take place to some extent. This is clearly not observed. Instead, the texture intensity is retained and even increased in some cases. Second, the grain size in the area where the highest deformation is achieved during blow forming is similar than in the non-deformed areas. The operation of GBS usually leads to concurrent grain growth [25]. Grain size stabilization during deformation might be attributed to the formation of new boundaries as a consequence of dislocation interaction. Third, the deformation conditions (stress, strain rate) are within the transition between the GBS-dominated regime and the CS dominated regime (Fig. 6).

The simultaneous occurrence of crystallographic slip and grain boundary sliding has been previously observed in Mg-Al alloys deformed in tension under similar conditions of temperature and strain rate [26]. In fact, the enhanced ductility of Mg-Al alloys with grain sizes larger 10 μm, a rather coarse grain for grain boundary sliding to produce large strains without failure due to cavitation, has been attributed to the

combined action of GBS and CS. The role of grain boundary sliding would be to cause random rotation of grains, accommodated by grain boundary diffusion. Simultaneously, at the high deformation temperatures used (~0.6 Tm), grain growth takes place. Enhanced grain growth contributes to a decrease in the grain boundary area and to a more difficult accommodation of the stresses caused by GBS at triple points. However, intragranular dislocation movement leads simultaneously to grain subdivision by the formation of geometrically necessary boundaries (GNBs). A balance between grain growth and grain subdivision is reached, leading ultimately to large tensile elongations before failure. The operation of each mechanism individually would lead to early fracture due either to cavity formation and coalescence (in the case of GBS) or to intergranular strain incompatibilities (if CS would operate alone). GBS and CS have also been observed to operate jointly in superplastic Al alloys when the corresponding testing conditions lie close to the transition region between the GBS-dominated regime (low strain rates-low stresses) and the CS-dominated regime [27]. Other metallic systems where GBS and CS have been reported to operate simultaneously are Zn alloys and INCONEL 718 [28-30].

In summary, superplastic forming of Mg alloys at an industrial level may only become a widespread technology once these materials can be formed under certain conditions of temperature ($T < 500ºC$), stress ($\sigma \leq 1$ MPa) and strain rate (around 10^{-3} s^{-1} or higher) [21]. Designing presses that can operate at higher stresses becomes very difficult, especially when forming large parts. Thus, in order to keep the stress levels within the allowed values, usually rather high temperatures (around 400ºC) must be used. Under these temperatures, as shown in the present study, grain growth takes place. Thus, grain refinement processing routes that lead to grain sizes below ~ 15 μm are

rendered unnecessary. However, the present investigation demonstrates that Mg-Al alloys may attain good superplastic formability even when their grain size is larger than 15 μm. This occurs at the expense of reducing the strain rate to values that are smaller than optimum (5×10^{-4} s^{-1} vs. 10^{-3} s^{-1}).

4. Conclusions

The aim of this study was to evaluate the superplastic formability of AZ31 and AZ61 Mg-Al alloys with various initial microstructures. Several thermomechanical processing routes including annealing, conventional rolling, severe rolling and cross rolling were utilized to fabricate a wide array of microstructures, with grain sizes ranging from 2 to 28 microns, and various grain shapes. The resulting materials were blow-formed into a hat-shaped die. It was found that, in order to keep the blow forming pressures within the permitted values (σ_{max}~ 1 MPa), optimum formability is obtained at rather high temperatures (400º C). Under these circumstances, significant grain size takes place already during heating to attain the forming temperature. Thus, the effect of the previous thermomechanical processing routes fades away and grain refinement procedures leading to very fine grain sizes (smaller than ~ 15 μm) are rendered unnecessary. Fortunately, the coexistence of grain boundary sliding and crystallographic slip in Mg-Al alloys during deformation at temperatures around 400º C, even when the initial grain sizes are larger than 15 microns, allows these materials to attain excellent superplastic formability at strain rates only somewhat lower than the optimum values.

Acknowledgments

The authors are thankful to Comunidad de Madrid for funding this work under grant GR-MAT-0715-2004. FS is grateful to CSIC for a postgraduate grant. JAV acknowledges support from a Ramón y Cajal contract awarded by the Spanish Ministry of Education and Science.

References

1. M. P. Staiger, A. M. Pietak, J. Huadmai and G. Dias: Biomaterials, 2006, 27, 1728–1734.
2. M. O. Pekguleryuz and A. A. Kaya: Adv. Eng. Mater., 2003, 5, 866–878.
3. H. Alves, U. Koster, E. Aghion and D. Eliezer: Mater. Technol., 2001, 16, 110–126.
4. A. A. Luo: Int. Mater. Rev., 2004, 49, 13–30.
5. C. J. Bettles and M. A. Gibson: Adv. Eng. Mater., 2003, 5, 859–865.
6. H. Kaufman and P. J. Uggowitzer: Adv. Eng. Mater., 2001, 3, 963–967.
7. M. Bamberger: Mater. Sci. Technol., 2001, 17, 15–24.
8. G. I. Rosen, G. Segal and A. Lubinski: Mater. Sci. Forum, 2005, 488–489, 509–513.
9. K. P. Park, M. J. Birt and K. J. A. Mawella: Adv. Perform. Mater.,1996, 3, 365–375.
10. T. G. Nieh, J. Wadsworth and O. D. Sherby: 'Superplasticity in metals and ceramics'; 1997, Cambridge, Cambridge University Press.
11. R. I. Todd: Mater. Sci. Technol., 2000, 16, 1287–1294.
12. Y. Miyahara, K. Matsubara, Z. Horita and T. G. Langdon: Metall. Mater. Trans. A, 2005, 36A, 1705–1711.
13. C. Xu, Z. J. Horita, M. Furukawa and T. G. Langdon: J. Mater. Eng. Perform., 2004, 13, 683–690.
14. T. Mukai, H. Watanabe and K. Higashi: Mater. Sci. Forum, 2000, 350–351, 159–170.
15. H. Hosokawa, Y. Chino, K. Shimojima, Y. Yamada, C. Wen, M. Mabuchi and H. Iwasaki: Mater. Trans., 2003, 44, 484–489.
16. L. C. Tsao, C. F. Wu and T. H. Chuang: Zeitschrift fur Metallkunde, 2001, 92, 572–577.
17. Y. Chino, M. Kobata, K. Shimojima, H. Hosokawa, Y. Yamada, H. Iwasaki and M. Mabuchi: Mater. Trans., 2004, 45, (2), 361–364.
18. A. Takara, Y. Nishikawa, H. Watanabe, H. Somekawa, T. Mukai and K. Higashi: Mater. Trans., 2004, 45, (8), 2531–2536.
19. S. W. Chung, W. J. Kim and K. Higashi: Mater. Sci. Forum, 2003, 419–422, 539–544.
20. A. W. El-Morsy, K. Manabe and H. Nishimura: Mater. Trans., 2002, 43, (10), 2443–2448.
21. T. R. McNelley: private communication, 2006.
22. J. A. del Valle, M. T. Pérez-Prado and O. A. Ruano: Mater. Sci. Eng. A, 2003,

23. D. A. Hughes and N. Hansen: Acta Mater., 1997, 45, 3871–3886.
24. H. J. Bunge: 'Texture analysis in materials science' ; 1982, London, Butterworths.
25. C. H. Cáceres and D. S. Wilkinson: J. Mater. Sci. Lett., 1984, 3, 395–399.
26. J. A. del Valle, M. T. Pérez-Prado and O. A. Ruano: Metall. Trans. A, 2005, 36A, (6), 1427–1438.
27. M. T. Pérez-Prado, T. R. McNelley, D. L. Swisher, G. González-Doncel and O. A. Ruano: Mater. Sci. Eng. A, 2003, A342, 216–230.
28. M. Urdanpilleta, J. M. Martínez-Esnaola and J. G. Sevillano, Mater. Trans., 2005, 46, (7), 1711–1719.
29. H. Brunner and N. J. Grant: Trans. AIME, 1960, 218, 122–127.
30. R. Z. Valiev and O. A. Kaibyshev: Acta Metall., 1983, 31, 2121–2128.

Figures

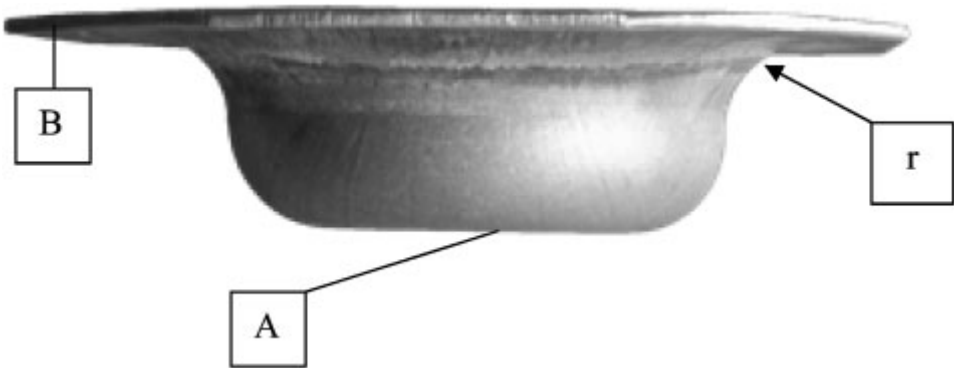

Figure 1. Profile of the blow formed specimens. Areas where cavity and grain growth measurements were performed.

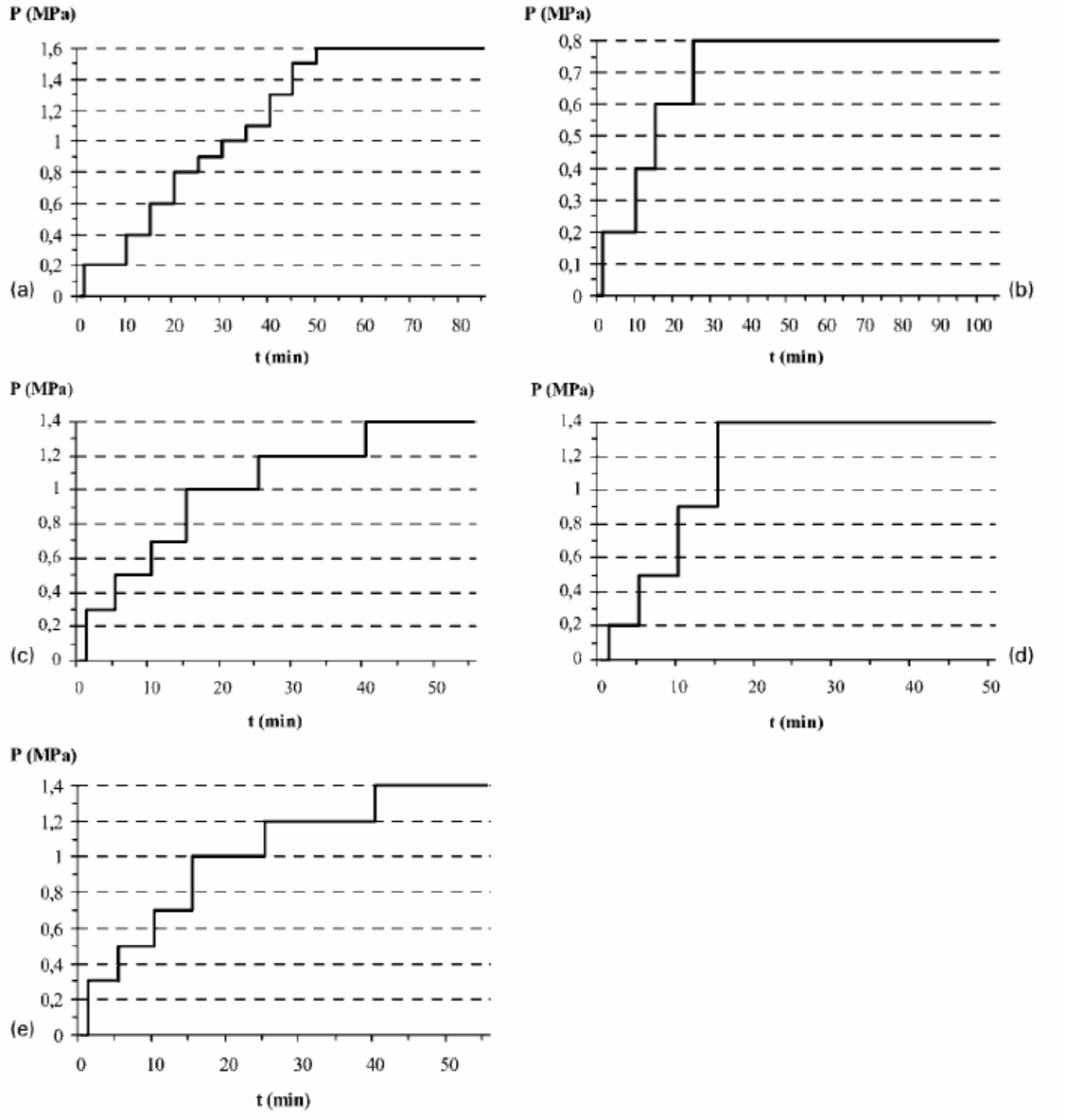

Figure 2: (a) cycle A (AZ31-O); (b) cycle B (AZ31-H); (c) cycle C (AZ31-SR); (d) cycle D (AZ61-SR); (e) cycle E (AZ61-CR) Pressure–time curves of different cycles used: T = 400 ^{o}C; r = 9 mm

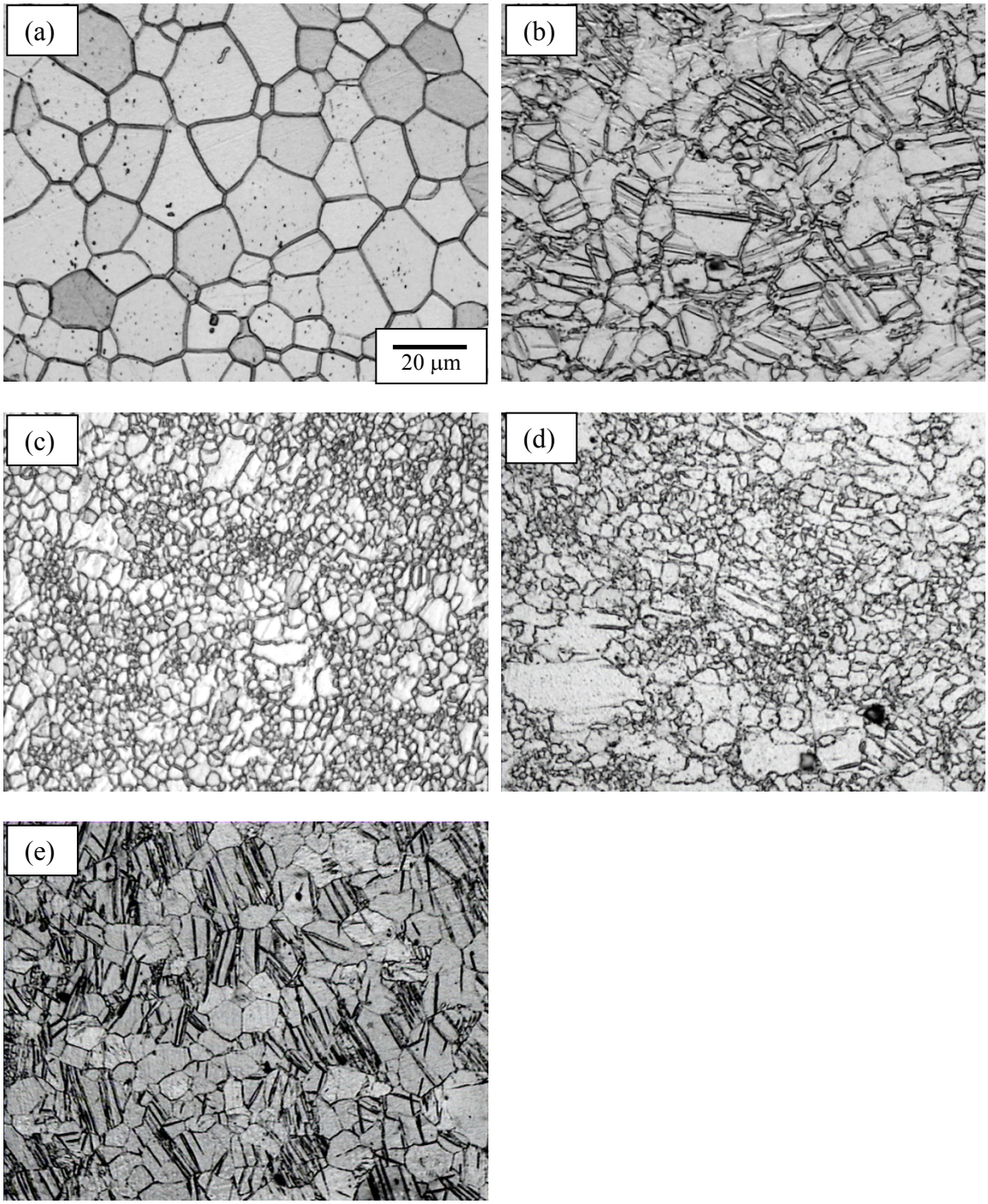

Figure 3. Initial microstructures: (a) AZ31-O, (b) AZ31-H, (c) AZ31-SR, (d) AZ61-SR, and (e) AZ61-CR.

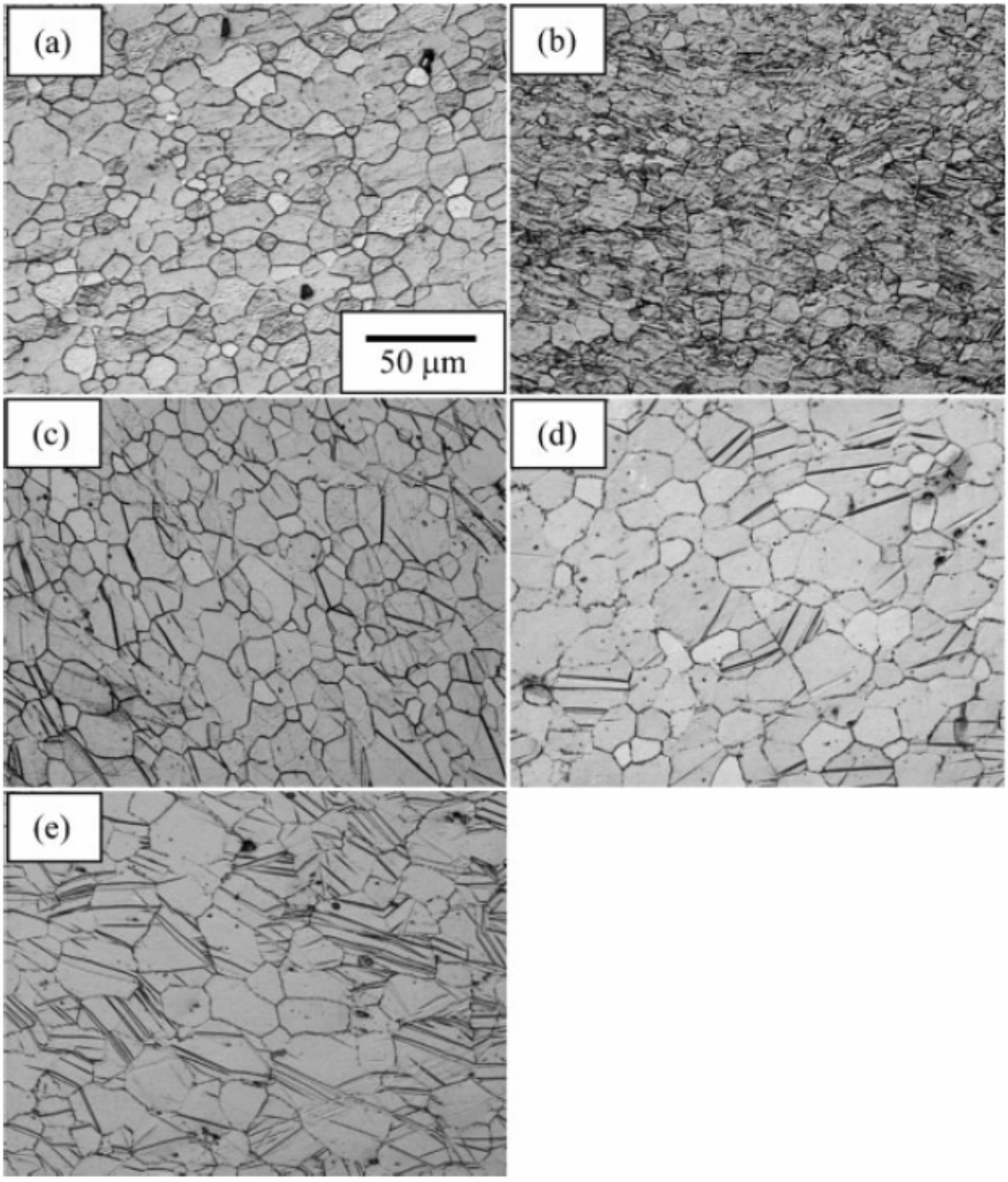

Figure 4: Microstructure of blow formed samples: (a) AZ31-O; (b) AZ31-H; (c) AZ31-SR; (d) AZ61-SR; (e) AZ61-CR

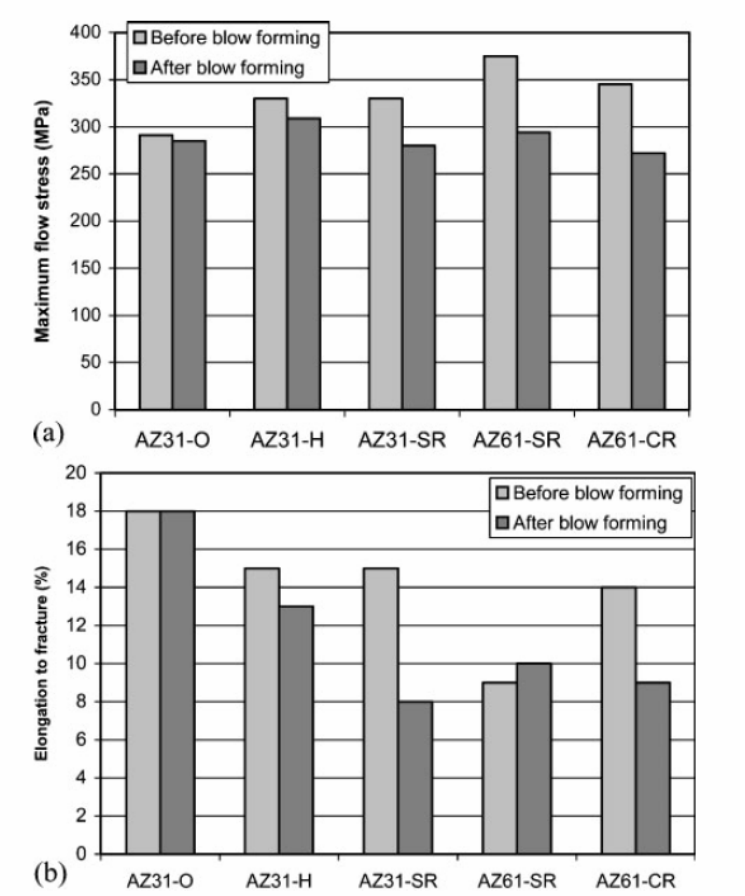

Figure 5. Comparison of the mechanical properties corresponding to the different Mg-Al alloys before and after blow forming. (a) Maximum flow stress; (b) Elongation.

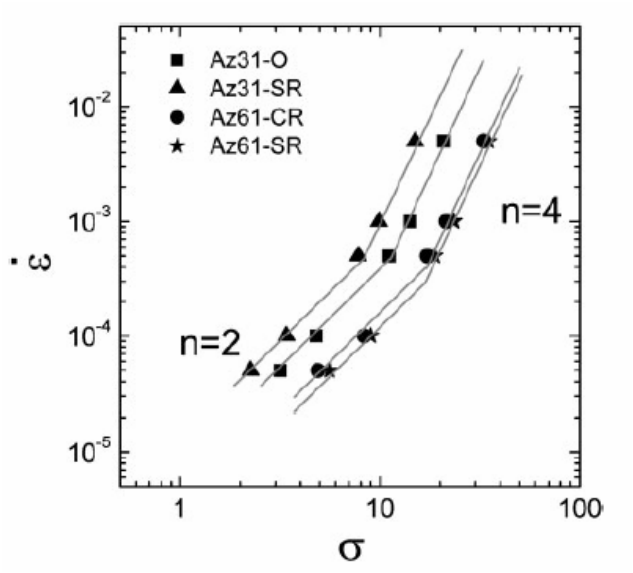

Figure 6. Strain rate vs. stress data from strain rate change tests performed at 400ºC.

Tables

Material	AZ31-O	AZ31-H	AZ31-SR	AZ61-SR	AZ61-CR
Temperature, °C	400	400	400	400	400
Radius, mm	9	9	9	9	9
Max. pressure, MPa	1·6	0·8	1·4	1·4	1·4
Forming time, min	85	105	55	50	55
Pressure–time*	Cycle A	Cycle B	Cycle C	Cycle D	Cycle E

Table 1. Blow forming conditions corresponding to the samples that exhibited optimum formability

Material	Grain size, μm	Microstructure type	Intensity of the basal fibre (times random)
AZ31-O	17	Equiaxed recrystallised	9
AZ31-H	7	Deformed coarse grains with twins	8
AZ31-SR	2 (small)–7 (coarse)	Bimodal coarse grains + small dynamically RX grains	8
AZ61-SR	2 (small) –20 (coarse)	Bimodal coarse grains + small dynamically RX grains	8
AZ61-CR	28	Equiaxed grains with a large fraction of twins	7

Table 2 Microstructure of as received and as processed (rolled) materials. In the calculation of grain size in the AZ31-H alloy twin boundaries have been included

Material	Area fraction of cavities, %		Grain size (in the blow formed samples), μm		Grain size (in the annealed materials), μm	Intensity of the basal fibre (times random)
Zone	A	B	A	B	–	A
AZ31-O	0·9	0·5	31	34	19	11
AZ31-H	0·5	0·5	18	14	18	8
AZ31-SR	0·3	0·0	31	31	17	10
AZ61-SR	0·7	0·2	41	42	33	7
AZ61-CR	2·8	0·3	41	41	36	7

Table 3 Microstructure of blow formed samples that exhibited optimum formability (see specific forming conditions in Table 1)